Optical Chirality in Nonlinear Optics: Application to High Harmonic Generation

Ofer Neufeld* and Oren Cohen†
Solid State Institute and Physics department, Technion—Israel Institute of Technology, Haifa 32000, Israel

(Received 13 September 2017; published 30 March 2018)

Optical chirality (OC)—one of the fundamental quantities of electromagnetic fields—corresponds to the instantaneous chirality of light. It has been utilized for exploring chiral light-matter interactions in linear optics, but has not yet been applied to nonlinear processes. Motivated to explore the role of OC in the generation of helically polarized high-order harmonics and attosecond pulses, we first separate the OC of transversal and paraxial beams to polarization and orbital terms. We find that the polarization-associated OC of attosecond pulses corresponds approximately to that of the pump in the quasimonochromatic case, but not in the multichromatic pump cases. We associate this discrepancy with the fact that the polarization OC of multichromatic pumps vary rapidly in time along the optical cycle. Thus, we propose new quantities, noninstantaneous polarization-associated OC, and time-scale-weighted polarization-associated OC, and show that these quantities link the chirality of multichromatic pumps and their generated attosecond pulses. The presented extension to OC theory should be useful for exploring various nonlinear chiral light-matter interactions. For example, it stimulates us to propose a tricircular pump for generation of highly elliptical attosecond pulses with a tunable ellipticity.

DOI: 10.1103/PhysRevLett.120.133206

Introduction.—Optical chirality (OC), a quantity that measures the local and instantaneous density of chirality of electromagnetic (EM) waves, is a very useful concept in light-matter interactions [1,2]. For example, it has been used for proposing "superchiral" fields (i.e., fields with a larger OC than circularly polarized fields) that yield ultradichroic interactions with chiral molecules [3,4]. However, OC has not yet been applied to chiral nonlinear optical processes. The reported results follow our motivation to explore the role of OC in the generation of helically polarized high harmonics.

In high harmonic generation (HHG) [5–7], intense ultrashort laser pulses are spectrally upconverted to the extreme UV and x-ray spectral regions. The process has been utilized for various applications, including the production of attosecond pulses [8], high resolution imaging [9–11], and probing the dynamics of electronic wave functions [12]. In HHG, electrons are first tunnel ionized, and are then accelerated by the intense laser field until they recombine with the ion and emit high harmonic radiation [6]. The trajectories of the recombining electrons can generally have durations on the same order of magnitude as that of the optical cycle of the driver, making this process noninstantaneous. In the "standard" geometry, HHG is driven by, and results with, linearly polarized light (i.e., with zero OC). Recently, generation and applications of highly helically polarized bright high harmonics were demonstrated experimentally [13–21]. Also, HHG from chiral media was shown to be chirality sensitive [22–24]. Given these exciting developments, it is pertinent to apply the concept of OC to HHG. For example, identifying correspondences between the OCs of the pump and high harmonic fields should lead to improved understanding and control of chiral HHG and attosecond pulses [25–30].

Here, we first divide the OC of transversal and paraxial beams to polarization and orbital terms, i.e., contributions from spin angular momentum (SAM) and orbital angular momentum (OAM). For the case where the polarization term is dominant, we develop a formalism for noninstantaneous OC and apply it for analyzing helical HHG. We discover that the chirality of HHG emission driven by a multispectral pump corresponds to a time-scale-weighted OC of the pump, which is comprised of both instantaneous and noninstantaneous chiralities. Stimulated by the new formalism, we propose a tricircular laser field that exhibits the required dynamical symmetry for generation of circularly polarized high harmonics (just like the bicircular field), and simultaneously it is unidirectionally chiral at all time scales (denoted a unichiral field). We show that such a field can produce chiral attosecond pulses, even from completely isotropic media, like helium gas. Furthermore, we show that the polarization and chirality of the attosecond pulses can be controlled by varying the time-scale-weighted OC of the tricircular fields. Lastly, we identify that OC is a robust quantity for estimating the circularity of few cycle pulses, where standard definitions such as ellipticity are ambiguous.

Polarization and orbital optical chirality.—The OC of an EM field in vacuum is given by [2]

$$C = \frac{\varepsilon_0}{2}\vec{E}\cdot\vec{\nabla}\times\vec{E} + \frac{1}{2\mu_0}\vec{B}\cdot\vec{\nabla}\times\vec{B}, \tag{1}$$

 © 2018 American Physical Society

where we use MKS. We first derive the polarization related terms in C for transversal and paraxial EM beams, denoted C_p. Mathematically, we neglect the z component and transverse derivatives of the EM field in Eq. (1), which yields

$$C_p = \frac{\varepsilon_0}{2}(E_y\partial_z E_x - E_x\partial_z E_y) + \frac{1}{2\mu_0}(B_y\partial_z B_x - B_x\partial_z B_y). \tag{2}$$

Assuming the pulses have a slowly varying envelope (SVE) along the z axis, we replace the z derivatives by time derivatives, yielding,

$$C_p = \frac{\varepsilon_0}{2c_0}(E_y\partial_t E_x - E_x\partial_t E_y) + \frac{1}{2c_0\mu_0}(B_y\partial_t B_x - B_x\partial_t B_y), \tag{3}$$

where c_0 is the speed of light in vacuum. Direct algebraic manipulation (see Appendix A) leads to

$$C_p = \frac{\varepsilon_0}{2c_0}|\vec{E}|^2\partial_t\phi(t) + \frac{1}{2c_0\mu_0}|\vec{B}|^2\partial_t\left(\phi(t)+\frac{\pi}{2}\right), \tag{4}$$

where $\phi = \tan^{-1}(E_y/E_x)$ is the angle of the electric field vector (the magnetic field vector is rotated by $\pi/2$). Labeling $\phi'(t)$ as the time derivative of ϕ, and $I = (c_0\varepsilon_0/2)|\vec{E}|^2 + (c_0/2\mu_0)|\vec{B}|^2$ the light intensity, Eq. (4) gets a compact and intuitive form:

$$C_p = \frac{1}{{c_0}^2}\phi\prime(t)I(t). \tag{5}$$

That is, the polarization-associated OC of paraxial beams corresponds to the product of the field's rotational velocity weighted by its intensity. This definition is an instantaneous measure for the chirality since both $\phi'(t)$ and $I(t)$ are evaluated at time t. Notably, OC is a dimensionful quantity that depends on the pulse envelope and frequency. Here we normalize polarization-associated OC to give a dimensionless quantity with respect to a circularly polarized pulse of a similar envelope and carrier frequency, such that for monochromatic waves, the instantaneous chirality coincides with the definition of ellipticity. For example, for an EM field with a fundamental frequency ω, a dimensionless envelope function $A(t)$, and a maximal amplitude E_0, the normalized polarization term of the OC is

$${C_p}^{\text{norm}} = \frac{\phi'(t)I(t)}{c_0\varepsilon_0|E_0|^2\omega\frac{1}{\tau}\int_0^\tau|A(t)|^2dt}, \tag{6}$$

where τ is the length of the pulse, and in the CW case the integral in the denominator vanishes to unity.

For completeness, we also derive the orbital term of the OC, denoted C_l. Starting with Eq. (1), assuming a beam with a SVE and neglecting the C_p term leads to

$$C_l = \frac{\frac{\varepsilon_0}{2}(E_x\partial_y E_z - E_z\partial_y E_x + E_z\partial_x E_y - E_y\partial_x E_z) + \frac{1}{2\mu_0}(B_x\partial_y B_z - B_z\partial_y B_x + B_z\partial_x B_y - B_y\partial_x B_z)}{}. \tag{7}$$

An algebraic manipulation [similar to the one leading to Eq. (4)] leads to

$$C_l = \frac{1}{c_0}(I_{xz}\partial_y\phi_{xz} - I_{yz}\partial_x\phi_{yz}), \tag{8}$$

where we have defined planar EM field intensities $I_{iz} = (c_0\varepsilon_0/2)(|E_i|^2 + |E_z|^2) + (c_0/2\mu_0)(|B_i|^2 + |B_z|^2)$ and planar angles $\phi_{iz} = \tan^{-1}(E_z/E_i)$, and "$i$" is the index for x or y axes. Employing the beam's paraxiality, C_l is well approximated by

$$C_l = \frac{1}{c_0}\left[I_x\partial_y\left(\frac{E_z}{E_x}\right) - I_y\partial_x\left(\frac{E_z}{E_y}\right)\right]. \tag{9}$$

Equation (9) clearly represents the orbital contribution to OC, as it is nonzero for linearly polarized fields, and measures the spatial rotation of the field in the transverse plane.

We are motivated to explore the generation of helically polarized HHG and therefore consider below only the polarization term of the OC. Thus, the index "p" is dropped henceforth, and any reference to OC relates to the polarization-associated term.

Optical chirality in HHG.—First, we explore HHG driven by quasimonochromatic elliptically polarized pumps [31,32], with an ellipticity ε. The HHG calculations (performed within the dipole approximation) are detailed in Appendix B. As shown in Fig. 1, the OC of the high harmonic field corresponds well to the OC of the driving laser, even though HHG is a highly nonlinear process [33].

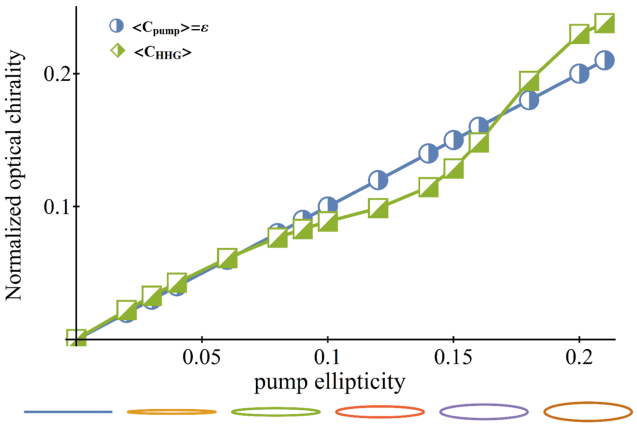

FIG. 1. Correlation of instantaneous OC of the driving monochromatic elliptical pump (which in this case is identically its ellipticity, ε) with numerically calculated time-averaged chirality of the emitted radiation, for $I_{\max} = 3\times10^{14}$ W/cm^2, $\lambda = 800$ nm. Bottom shows the parametric Lissajou curve of the driver as the ellipticity is increased.

Next, we consider HHG driven by ω-2ω bicircular fields with equal amplitudes [13,14,18–21,34–36]. In this case, the OC of the pump varies from 0 to 0.5, and its average is $\langle C_{\text{pump}} \rangle = 0.25$ [see Figs. 2(a) and 2(b)]. The emitted attopulses, on the other hand, are generally not helical [30,37,38]; i.e., their OC is approximately zero. This discrepancy is not a surprise since HHG is a nonlinear noninstantaneous process; hence, it is not guaranteed that there is any correspondence between the (instantaneous) OC of the pump and HHG field. Still, motivated to correlate the OC of the HHG field with the pump chirality, we propose quantities that describe the non-instantaneous OC (the inherent duration of HHG corresponds to the time interval of the electron's motion in the continuum, which is typically in the range of ¼–¾ of the duration of the pump's optical cycle).

Noninstantaneous optical chirality—To include noninstantaneous effects for a given time scale, we alter Eq. (5) to

$$\chi(t, \Delta t) = \frac{1}{{c_0}^2} \frac{\phi(t + \Delta t) - \phi(t)}{\Delta t} \bar{I}(t, \Delta t), \tag{10}$$

where $\bar{I}(t, \Delta t) = 0.5[I(t) + I(t + \Delta t)]$. Equation (10) introduces chirality by time scale $\chi(t, \Delta t)$ and reduces to Eq. (5) for $\Delta t = 0$. Furthermore, we propose a time-scale-weighted OC, $\chi_{\text{tot}}(t)$, for analyzing processes with multiple time scales:

$$\chi_{\text{tot}}(t) = \int_{\Delta t=0}^{\Delta t_{\text{cutoff}}} w_{\Delta t} \chi(t, \Delta t) d(\Delta t), \tag{11}$$

where $w_{\Delta t}$ is a weighting coefficient indicating the contribution of the time scale Δt to the overall chirality, and Δt_{cutoff} is a cutoff for the time scales. It may be possible to derive the weighting and cutoff coefficients in Eq. (11) from models describing the specific nonlinear process. Here, we take a simplified approach and assume that the two dominant time scales are $\Delta t = 0$ and another Δt that (i) reflects the time scale of the nonlinear process (e.g., duration of the re-colliding electron trajectory in HHG), and (ii) corresponds to the duration of the dynamical symmetry of the driving pulse [i.e., the chirality by time scale, $\chi(t, \Delta t)$, gets strong maxima in these delays].

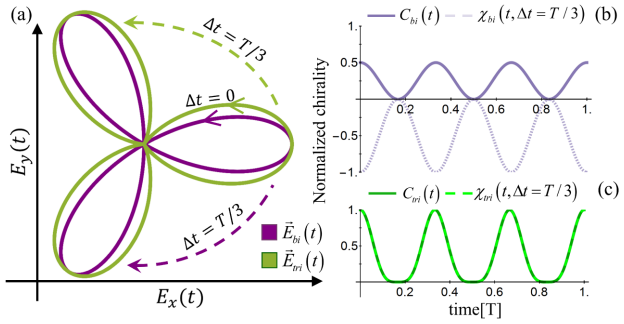

FIG. 2. Optical chirality of bicircular and tricircular fields, at intensity ratios 1:1 and 2:1:1, respectively. (a) Lissajou of the bicircular (purple) and tricircular (green) fields. Full arrows represent the instantaneous motion of the field, dashed arrows represent motion on $T/3$ time scales. The instantaneous and long motions are unidirectional for the tricircular field while they have opposite directions in the bicircular fields. (b) Instantaneous and non-instantaneous (for $\Delta t = T/3$) optical chiralities of bicircular pump. (c) Same as (b), but for tricircular pump, where $C_{\text{tri}}(t)$ and $\chi_{\text{tri}}(t, \Delta t = T/3)$ coincide.

Noninstantaneous optical chirality in HHG.—We now employ the noninstantaneous chirality formalism to analyze the generation of helical attopulses driven by multispectral pumps.

First, we explore a counterrotating ω-2ω bicircular pump

$$\vec{E}_{\text{bi}}(t) = E_1 \hat{e}_R e^{i\omega t} + E_2 \hat{e}_L e^{2i\omega t}, \tag{12}$$

where $\hat{e}_{R/L}$ represents a right-left circularly polarized field vector, ω is the optical frequency related to the field's period, $T = 2\pi/\omega$, and $E_{1,2}$ are the field amplitudes. Because of its threefold rotational symmetry, this field generates circular high harmonics with an alternating helicity [13,14,39]. Even though the bicircular driver produces circular harmonics, it often leads to an overall nonchiral response, and linearly polarized attopulses [30,37,38]. Applying Eq. (10) on the bicircular field at intensity ratios $E_1 = E_2$ (1:1), we find $\langle \chi(t, \Delta t = 0) \rangle = 0.25$ and $\langle \chi(t, \Delta t = T/3) \rangle = -0.5$. That is, the bicircular field at this intensity ratio changes its helicity from shorter to longer time scales, which influences the HHG process. The resulting nonchiral response can then be intuitively understood as two opposing chiral time scales that average out during the electron's motion in the continuum. This argument suggests that in order to produce a significant chiral response in the medium, the driver should be corotating on these time scales (thus eliminating the opposing contributions to the chirality); hence, the driver should be unidirectional at all time scales [i.e., $\chi(t, \Delta t) > 0$ for all $t, \Delta t$], denoted "unichiral." One can generate such a field without breaking the discrete threefold dynamical symmetry by adding a third circular field at frequency 4ω to the bicircular scheme, which we denote the tricircular scheme:

$$\vec{E}_{\text{tri}}(t) = E_1 \hat{e}_R e^{i\omega t} + E_2 \hat{e}_L e^{2i\omega t} + E_4 \hat{e}_R e^{4i\omega t}. \tag{13}$$

For $E_4 = 0$ the pump in Eq. (13) reduces to the bicircular pump. The addition of a 4th harmonic term tilts the balance of helicity in favor of anticlockwise rotation. Tuning the intensity ratios in Eq. (13) ($E_1 : E_2 : E_4$) allows manipulating the OC on multiple time scales. For comparison, at intensity ratios 2:1:1, the tricircular field has a very similar shape to the bicircular field at intensity ratios 1:1, but is unichiral, and rotates anticlockwise on all time scales [Figs. 2(a) and 2(c)].

We numerically show that this configuration generates a chiral response from an isotropic medium on a single atom level from an initial $1s$ state (see Appendix B for numerical details). Filtering out below ionization potential (Ip) harmonics yields a highly helical attopulse train [Fig. 3(b)] with an averaged OC of 0.64 (equivalent to an ellipticity of 0.66), as opposed to the bicircular field that generates a linearly polarized attopulse train with an averaged OC of 0.08 [Fig. 3(a)]. From a spectral point of view, even though the tricircular driver generates both left and right circular harmonics, the intensity of each right rotating harmonic is about 5 times larger than that of the nearby left rotating harmonic. The main difference between the driving fields is the long-term rotation directionality, indicating that the noninstantaneous chirality of the pump leads to the drastic change in the emitted radiation's chirality. The drawbacks for adding the 4ω field are reductions in cutoff energy and conversion efficiency (by 1 order of magnitude), which is consistent with the Coriolis force model [40,41] for HHG driven by bichromatic corotating pulses.

Next, we investigate a wider range of intensity ratios in the tricircular scheme and examine the correspondence between the chirality of light emitted from HHG to the chirality of the driver. We define a parameter η which is varied from 0 to 1 as the tricircular field changes its intensity ratios from 1:1:0, to 2:1:1. The pump then has the form

$$\vec{E}_{\mathrm{tri},\eta}(t) = E_{0,\eta}[(1+\eta)\hat{e}_R e^{i\omega t} + \hat{e}_L e^{2i\omega t} + \eta\hat{e}_R e^{4i\omega t}], \quad (14)$$

where $E_{0,\eta}$ is normalized per η to keep the peak amplitude constant. The spatiotemporal shape of this field is shown for several values of η in the bottom of Fig. 4. For each value of η we calculate the OC of the emitted radiation. Figure 4 clearly shows that varying the intensity ratios in the driver tunes the chirality of the emitted light. As discussed above, the instantaneous OC of the pump generally does not correspond to the instantaneous OC of the high harmonic waves. For example, for $\eta = 0.3$ the time-averaged OC of the driver is $\langle C_{\mathrm{pump}}\rangle = 0$, while the emitted light is chiral ($\langle C_{\mathrm{HHG}}\rangle > 0$). Also, for $\eta = 0.2$, the OC of the driver is negative ($\langle C_{\mathrm{pump}}\rangle < 0$), while that of the emitted light is positive ($\langle C_{\mathrm{HHG}}\rangle > 0$). We approximate the time-scale-weighted optical chirality of the driver with Eq. (11) as comprised from just two time scales, $\Delta t = 0$ and $\Delta t = T/3$:

$$\langle \chi_{\mathrm{tot}}\rangle \approx w_0\langle \chi(t,0)\rangle + w_{T/3}\langle \chi(t,T/3)\rangle. \quad (15)$$

We search for a correspondence between the time-scale-weighted OC of the pump to the instantaneous OC of the HHG field to derive the weighting coefficients. A best fit is found for $w_0 = 2.14 w_{T/3}$, with $R^2 = 0.993$ (Fig. 4), from which we can gain some physical intuition on the system at hand: in tricircular HHG the instantaneous time scale is more significant than the $T/3$ time scale. Similar results are also obtained for a fourfold symmetric tricircular pump with frequencies ω-3ω-5ω, where the $T/4$ time scale plays a significant role (see Appendix C).

We also applied the OC approach for investigating attopulses generated by the bicircular scheme with varying amplitude ratios. This scheme was proposed and implemented experimentally to produce highly chiral overall HHG spectra [30], which should also correspond to attosecond pulses with large ellipticity (the first experimental highly chiral overall HHG spectra using bicircular pumps

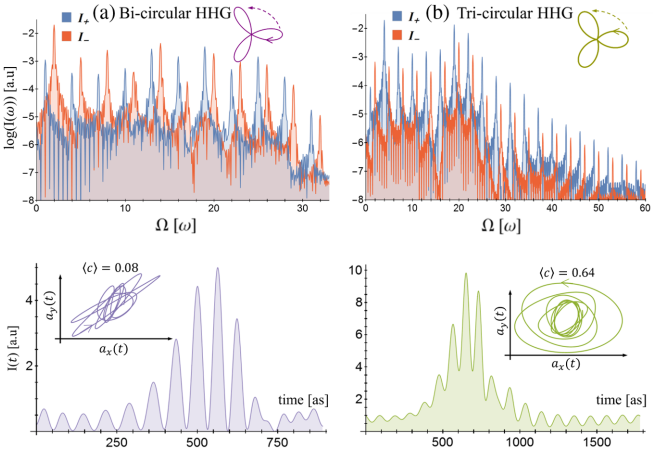

FIG. 3. Numerical HHG spectral intensity projected onto left and right rotating components in log scale (top) and emitted attopulse trains (bottom) from (a) bicircular ω-2ω driver with intensity ratios 1:1, $I_{\max} = 2\times10^{14}$ W/cm^2, $\lambda = 800$ nm, (b) unichiral tricircular ω-2ω-4ω driver with intensity ratios 2:1:1, $I_{\max} = 3\times10^{14}$ W/cm^2, $\lambda = 1600$ nm. Top inset shows a Lissajou curve of the driver, and bottom inset a Lissajou curve of a single burst of the emitted attopulse train.

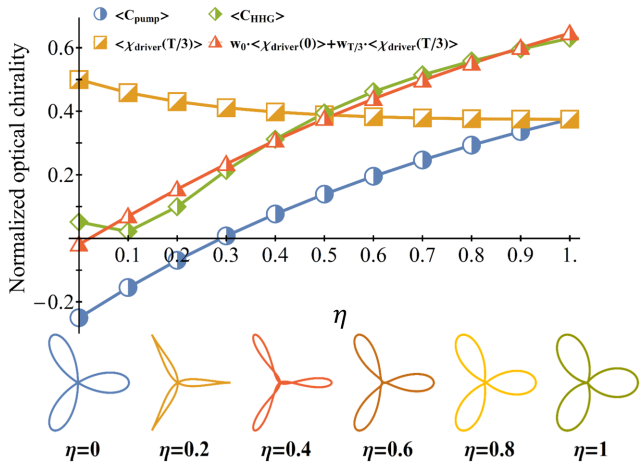

FIG. 4. Correspondence between time-averaged noninstantaneous OC of the driving tricircular pump to the numerically calculated time-averaged OC of the emitted radiation, for $I_{\max} = 3\times10^{14}$ W/cm^2, $\lambda = 1600$ nm. Bottom shows the parametric Lissajou curve of the driver as η is varied. The best fit using two time scales is obtained for $w_0 = 2.14 w_{T/3}$, with an $R^2 = 0.993$ between the green and red curves.

was reported in Ref. [20]). In Ref. [30], the intensity ratios in the counterrotating bicircular field were tuned such that $I_\omega > I_{2\omega}$, which results in highly chiral attopulses. A symmetric manipulation of $I_{2\omega} > I_\omega$ leads to less chiral attopulses. The noninstantaneous OC theory elucidates that this occurs because for $I_\omega > I_{2\omega}$ one produces a unichiral pump, while for $I_{2\omega} > I_\omega$ the pump's instantaneous chirality is increased but remains opposite to its noninstantaneous chirality, resulting in a reduced chiral response (Fig. 5).

Interestingly, oscillations in the OC of emitted attopulses in Figs. 4 and 5 appear when the instantaneous and noninstantaneous chiralities of the pump are oppositely signed (the oscillations are larger in Fig. 5 because the difference between the instantaneous and noninstantaneous chiralities is larger). In this regime, the HHG field's chirality deviates from the approximated behavior of just two time-averaged chiral time scales.

Lastly, we note that a time-averaged OC ($\langle C \rangle$) provides a robust and effective quantity for estimating an EM field's degree of circularity, where standard definitions such as ellipticity can be ambiguous. Ellipticity becomes ambiguous if pulses are comprised of broadband spectra (such as in HHG), and the spatiotemporal profile of the pulse no longer resembles an ellipse. For instance, using stokes parameters [42] to calculate the "ellipticity" of an ω-2ω counterrotating bicircular field (at amplitude ratios 1:1) results in an ellipticity $\varepsilon = 1$, even though the field is clearly not "as circular" as circularly polarized light. Using OC gives a more realistic estimate of $\langle C \rangle = 0.25$, i.e., still circular, but less than circularly polarized light. This issue naturally also occurs in more complex wave forms that are comprised of multiple high harmonics; thus, we propose using the averaged OC to evaluate the circularity in these cases.

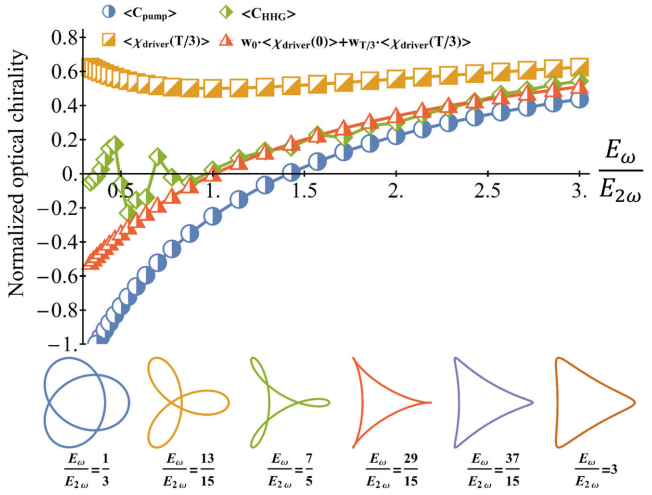

FIG. 5. Same as in Fig. 4, but for a bicircular pump [Eq. (12)] with varying amplitude ratios between its first and second harmonic, for $I_{\max} = 2.5 \times 10^{14}$ W/cm^2, $\lambda = 800$ nm. OC is calculated for emitted attopulses (below Ip harmonics are filtered out).

Summary.—We presented a noninstantaneous optical chirality theory, and used it to analyze multi-chromatic helical HHG. We first divided the OC of transverse and paraxial beams to polarization and orbital terms, and then extended polarization-associated OC to include noninstantaneous contributions. Our results show that the chirality of the emitted HHG field corresponds to both the instantaneous and noninstantaneous chiralities of the pump. We use this intuition to predict unichiral tricircular field configurations that are unidirectionally helical, and can drive highly helical attopulse trains from an isotropic medium. Moreover, the attopulses' polarization state can be controlled by tuning the time-scale-weighted chirality of the pump. Lastly, we recommended the use of averaged OC to evaluate the circularity of broadband ultrashort pulses.

This work paves the way to various new research directions. First, application of OC in other nonlinear optical processes may yield new insights. Second, the separation of OC to polarization (SAM) and orbital (OAM) terms allows investigating regimes where the terms are of similar magnitude and might interact, or convert from one to another, which may be applicable to HHG driven by beams carrying OAM [43]. Third, it will be interesting to apply the OC approach to HHG from anisotropic and chiral media (e.g., molecular gas [41] and solids [44]). For example, we expect that the use of uni-chiral fields in HHG would lead to enhanced selectivity of chiral HHG spectroscopy [22,23]. Four, OC theory is also applicable to strong-field ionization of atoms and molecules, and could be useful for producing and controlling electron vortices, rotational electron currents, and spin-polarized electrons [45–48]. Lastly, noninstantaneous OC and unichiral fields should prove useful for the production of intense ultrashort magnetic field pulses [49].

This work was supported by the Israel Science Foundation (Grant No. 1225/14), the Israeli Center of Research Excellence "Circle of Light" supported by the I-CORE Program of the Planning and Budgeting Committee and the Israel Science Foundation (Grant No. 1802/12), and the Wolfson foundation. O. N. gratefully acknowledges the support of the Adams Fellowship Program of the Israel Academy of Sciences and Humanities.

APPENDIX A: TRANSITION FROM EQ. (3) TO EQ. (4)

The transition from Eq. (3) to Eq. (4) uses the following identity, both on the electric and magnetic fields:

$$\begin{aligned}(F_y \partial_t F_x - F_x \partial_t F_y) &= (F_x{}^2 + F_y{}^2)\frac{1}{1+(\frac{F_y}{F_x})^2}\frac{(F_y \partial_t F_x - F_x \partial_t F_y)}{F_x{}^2} \\ &\equiv (F_x{}^2 + F_y{}^2)\frac{\partial}{\partial t}\left[\tan^{-1}\left(\frac{F_y}{F_x}\right)\right], \end{aligned} \tag{A1}$$

where $\vec{F}$ is a time-dependent vector.

APPENDIX B: HHG NUMERICAL DETAILS

Numerical calculations of the high harmonic spectrum were performed by solving the time-dependent 2D Schrödinger equation in the length gauge, within the single active electron approximation, and the dipole approximation. The system's time-dependent Hamiltonian is given in atomic units by

$$\mathscr{H}(t) = \left(-\frac{1}{2}\vec{\nabla}^2 + V_{\text{atom}}(\vec{r}) + \vec{r}\cdot\vec{E}_{\text{pulse}}(t)\right), \quad \text{(B1)}$$

where V_{atom} represents a spherically symmetric coulomb softened atomic potential well, set to describe the ionization potential of Ne ($I_p = 0.793$ a.u.) [27],

$$V_{\text{atom}}(\vec{r}) = -\frac{1}{\sqrt{\vec{r}^2 + 0.1195}}, \quad \text{(B2)}$$

$\vec{E}_{\text{pulse}}(t)$ is the electric field of the pump pulse, defined by the electric field of monochromatic elliptical, or multichromatic pumps as specified in the main text, respectively, times a flattop envelope function with a 4 fundamental cycle long rise and drop sections and a 6 cycle long flattop. The initial wave function was chosen as the atomic $1s$ ground state found by complex time propagation. The Schrödinger equation was discretized on a square real-space grid of size $L \times L$ for $L = 120$ a.u., with spacing $dx = dy = 0.2348$ a.u., and propagated with a 3rd order split operator method [50,51] with a time step $dt = 0.01$ a.u. Convergence was tested with respect to grid size, density, and time step. Absorbing boundaries were used with the absorber set to (in a.u.),

$$V_{ab}(\vec{r}) = -i5 \times 10^{-4}\Theta((|\vec{r}| - 36)^3), \quad \text{(B3)}$$

where Θ represents a Heaviside step function. The dipole acceleration was calculated using the Ehrenfest theorem [52], from which the harmonic spectrum is found by Fourier transform. The OC of the HHG field is calculated after removing the fundamental harmonics in the spectrum, and is normalized with respect to the OC of the most chiral attopulse train emitted from the given geometry (after filtering out below Ip harmonics).

APPENDIX C: FOURFOLD TRICIRCULAR PUMPS

This appendix presents a similar analysis as that in the text for tricircular ω-2ω-4ω pumps, but for a fourfold symmetric tricircular field comprised of the ω-3ω-5ω frequencies. This arrangement allows manipulating the chirality of the pump by tuning the intensity ratios between the different colors without breaking the fourfold symmetry. We define the same parameter η which is varied from 0 to 1, and the pump field varies as follows:

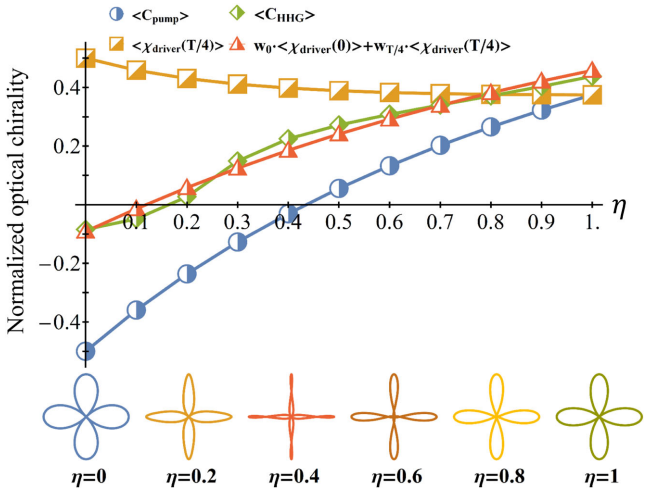

FIG. 6. Same as in Fig. 4, but for a tricircular fourfold symmetric field [Eq. (C1)], for $I_{\max} = 3 \times 10^{14}$ W/cm^2, $\lambda = 1600$ nm.

$$\vec{E}^{\text{fourfold}}_{\text{tri},\eta} = E_{0,\eta}[(1+\eta)\hat{e}_R e^{i\omega t} + \hat{e}_L e^{3i\omega t} + \eta\hat{e}_R e^{5i\omega t}]. \quad \text{(C1)}$$

The results are seen in Fig. 6, which shows a correspondence between the HHG field's instantaneous OC and both instantaneous and noninstantaneous contributions to the chirality, dominated by the $T/4$ time scale.

*ofern@tx.technion.ac.il
†oren@technion.ac.il

[1] D. M. Lipkin, J. Math. Phys. **5**, 696 (1964).
[2] Y. Tang and A. E. Cohen, Phys. Rev. Lett. **104**, 163901 (2010).
[3] Y. Tang and A. E. Cohen, Science **332**, 333 (2011).
[4] E. Hendry, T. Carpy, J. Johnston, M. Popland, R. V. Mikhaylovskiy, A. J. Lapthorn, S. M. Kelly, L. D. Barron, N. Gadegaard, and M. Kadodwala, Nat. Nanotechnol. **5**, 783 (2010).
[5] A. McPherson, G. Gibson, H. Jara, U. Johann, T. S. Luk, I. A. McIntyre, K. Boyer, and C. K. Rhodes, J. Opt. Soc. Am. B **4**, 595 (1987).
[6] P. B. Corkum, Phys. Rev. Lett. **71**, 1994 (1993).
[7] F. Krausz and M. Ivanov, Rev. Mod. Phys. **81**, 163 (2009).
[8] M. Hentschel, R. Kienberger, C. Spielmann, G. A. Reider, N. Milosevic, T. Brabec, P. Corkum, U. Heinzmann, M. Drescher, and F. Krausz, Nature (London) **414**, 509 (2001).
[9] R. L. Sandberg, A. Paul, D. A. Raymondson, S. Hädrich, D. M. Gaudiosi, J. Holtsnider, R. I. Tobey, O. Cohen, M. M. Murnane, H. C. Kapteyn, C. Song, J. Miao, Y. Liu, and F. Salmassi, Phys. Rev. Lett. **99**, 098103 (2007).
[10] M. D. Seaberg, D. E. Adams, E. L. Townsend, D. A. Raymondson, W. F. Schlotter, Y. Liu, C. S. Menoni, L. Rong, C. C. Chen, J. Miao, H. C. Kapteyn, and M. M. Murnane, Opt. Express **19**, 22470 (2011).
[11] O. Kfir, S. Zayko, C. Nolte, M. Sivis, M. Möller, B. Hebler, S. S. P. K. Arekapudi, D. Steil, S. Schäfer, M. Albrecht,

O. Cohen, S. Mathias, and C. Ropers, Sci. Adv. **3**, eaao4641 (2017).
[12] E. Goulielmakis, Z. H. Loh, A. Wirth, R. Santra, N. Rohringer, V. S. Yakovlev, S. Zherebtsov, T. Pfeifer, A. M. Azzeer, M. F. Kling, S. R. Leone, and F. Krausz, Nature (London) **466**, 739 (2010).
[13] A. Fleischer, O. Kfir, T. Diskin, P. Sidorenko, and O. Cohen, Nat. Photonics **8**, 543 (2014).
[14] O. Kfir, P. Grychtol, E. Turgut, R. Knut, D. Zusin, D. Popmintchev, T. Popmintchev, H. Nembach, J. M. Shaw, A. Fleischer, H. Kapteyn, M. Murnane, and O. Cohen, Nat. Photonics **9**, 99 (2015).
[15] A. Ferré, C. Handschin, M. Dumergue, F. Burgy, A. Comby, D. Descamps, B. Fabre, G. a. Garcia, R. Géneaux, L. Merceron, E. Mével, L. Nahon, S. Petit, B. Pons, D. Staedter, S. Weber, T. Ruchon, V. Blanchet, and Y. Mairesse, Nat. Photonics **9**, 93 (2015).
[16] G. Lambert, B. Vodungbo, J. Gautier, B. Mahieu, V. Malka, S. Sebban, P. Zeitoun, J. Luning, J. Perron, A. Andreev, S. Stremoukhov, F. Ardana-Lamas, A. Dax, C. P. Hauri, A. Sardinha, and M. Fajardo, Nat. Commun. **6**, 6167 (2015).
[17] D. D. Hickstein, F. J. Dollar, P. Grychtol, J. L. Ellis, R. Knut, C. Hernández-García, D. Zusin, C. Gentry, J. M. Shaw, T. Fan, K. M. Dorney, A. Becker, A. Jaroń-Becker, H. C. Kapteyn, M. M. Murnane, and C. G. Durfee, Nat. Photonics 2015) 743 ,**9**).
[18] T. Fan *et al.*, Proc. Natl. Acad. Sci. U.S.A. **112**, 14206 (2015).
[19] O. Kfir, E. Bordo, G. Ilan Haham, O. Lahav, A. Fleischer, and O. Cohen, Appl. Phys. Lett. **108**, 211106 (2016).
[20] O. Kfir, P. Grychtol, E. Turgut, R. Knut, D. Zusin, A. Fleischer, E. Bordo, T. Fan, D. Popmintchev, T. Popmintchev, H. Kapteyn, M. Murnane, and O. Cohen, J. Phys. B **49**, 123501 (2016).
[21] D. Baykusheva, M. S. Ahsan, N. Lin, and H. J. Wörner, Phys. Rev. Lett. **116**, 123001 (2016).
[22] R. Cireasa, A. E. Boguslavskiy, B. Pons, M. C. H. Wong, D. Descamps, S. Petit, H. Ruf, N. Thiré, A. Ferré, J. Suarez, J. Higuet, B. E. Schmidt, A. F. Alharbi, F. Légaré, V. Blanchet, B. Fabre, S. Patchkovskii, O. Smirnova, Y. Mairesse, and V. R. Bhardwaj, Nat. Phys. **11**, 654 (2015).
[23] O. Smirnova, Y. Mairesse, and S. Patchkovskii, J. Phys. B **48**, 234005 (2015).
[24] X. Zhu, X. Liu, P. Lan, D. Wang, Q. Zhang, W. Li, and P. Lu, Opt. Express **24**, 24824 (2016).
[25] K. J. Yuan and A. D. Bandrauk, Phys. Rev. A **84**, 023410 (2011).
[26] K. J. Yuan and A. D. Bandrauk, Phys. Rev. Lett. **110**, 023003 (2013).
[27] L. Medišauskas, J. Wragg, H. van Der Hart, and M. Y. Ivanov, Phys. Rev. Lett. **115**, 153001 (2015).
[28] P. C. Huang, C. H. Lu, C. Hernández-García, R. T. Huang, P. S. Wu, D. D. Hickstein, D. A. Thrasher, J. Ellis, A. H. Kung, S. D. Yang, A. Jaron-Becker, A. Becker, H. Kapteyn, M. M. Murnane, C. Durfee, and M. C. Chen, *Isolated, Circularly Polarized, Attosecond Pulse Generation* (Optical Society of America, San Jose, California, 2016), p. JTh4A.7.
[29] G. Lerner, T. Diskin, O. Neufeld, O. Kfir, and O. Cohen, Opt. Lett. **42**, 1349 (2017).
[30] K. M. Dorney, J. L. Ellis, C. Hernández-Garc'ia, D. D. Hickstein, C. A. Mancuso, N. Brooks, T. Fan, G. Fan, D. Zusin, C. Gentry, P. Grychtol, H. C. Kapteyn, and M. M. Murnane, Phys. Rev. Lett. **119**, 063201 (2017).
[31] T. Kanai, S. Minemoto, and H. Sakai, Phys. Rev. Lett. **98**, 053002 (2007).
[32] M. Möller, Y. Cheng, S. D. Khan, B. Zhao, K. Zhao, M. Chini, G. G. Paulus, and Z. Chang, Phys. Rev. A **86**, 011401 (2012).
[33] P. Antoine, B. Carré, A. L'Huillier, and M. Lewenstein, Phys. Rev. A **55**, 1314 (1997).
[34] H. Eichmann, A. Egbert, S. Nolte, C. Momma, B. Wellegehausen, W. Becker, S. Long, and J. K. McIver, Phys. Rev. A **51**, R3414(R) (1995).
[35] S. Long, W. Becker, and J. K. McIver, Phys. Rev. A **52**, 2262 (1995).
[36] T. Zuo and A. D. Bandrauk, J. Nonlinear Opt. Phys. Mater. **04**, 533 (1995).
[37] D. B. Milošević and W. Becker, Phys. Rev. A **62**, 011403(R) (2000).
[38] C. Chen, Z. Tao, C. Hernández-García, P. Matyba, A. Carr, R. Knut, O. Kfir, D. Zusin, C. Gentry, P. Grychtol, O. Cohen, L. Plaja, A. Becker, A. Jaron-Becker, H. Kapteyn, and M. Murnane, Sci. Adv. **2**, e1501333 (2016).
[39] O. E. Alon, V. Averbukh, and N. Moiseyev, Phys. Rev. Lett. **80**, 3743 (1998).
[40] F. M., A. D. B., T. Uzer, F. Mauger, A. D. Bandrauk, and T. Uzer, J. Phys. B **49**, 10LT01 (2016).
[41] A. D. Bandrauk, F. Mauger, and K.-J. Yuan, J. Phys. B **49**, 23LT01 (2016).
[42] W. H. McMaster, Am. J. Phys. **22**, 351 (1954).
[43] G. Gariepy, J. Leach, K. T. Kim, T. J. Hammond, E. Frumker, R. W. Boyd, and P. B. Corkum, Phys. Rev. Lett. **113**, 153901 (2014).
[44] S. Ghimire, A. D. DiChiara, E. Sistrunk, P. Agostini, L. F. DiMauro, and D. A. Reis, Nat. Phys. **7**, 138 (2011).
[45] I. Barth and O. Smirnova, Phys. Rev. A **88**, 013401 (2013).
[46] A. Hartung, F. Morales, M. Kunitski, K. Henrichs, A. Laucke, M. Richter, T. Jahnke, A. Kalinin, M. Schöffler, L. P. H. Schmidt, M. Ivanov, O. Smirnova, and R. Dörner, Nat. Photonics **10**, 526 (2016).
[47] D. Pengel, S. Kerbstadt, D. Johannmeyer, L. Englert, T. Bayer, and M. Wollenhaupt, Phys. Rev. Lett. **118**, 053003 (2017).
[48] S. Kerbstadt, D. Pengel, D. Johannmeyer, L. Englert, T. Bayer, and M. Wollenhaupt, New J. Phys. **19**, 103017 (2017).
[49] K. J. Yuan and A. D. Bandrauk, Phys. Rev. A **92**, 063401 (2015).
[50] J. A. Fleck, J. R. Morris, and M. D. Feit, Appl. Phys. **10**, 129 (1976).
[51] M. D. Feit, J. A. Fleck, and A. Steiger, J. Comput. Phys. **47**, 412 (1982).
[52] K. Burnett, V. C. Reed, J. Cooper, and P. L. Knight, Phys. Rev. A **45**, 3347 (1992).